Lecture 15: PDE-constrained optimization

AME60714: Advanced Numerical Methods

Matthew J. Zahr
Aerospace and Mechanical Engineering
University of Notre Dame

PDE optimization is ubiquitous in science and engineering

Design: Find system that optimizes performance metric, satisfies constraints

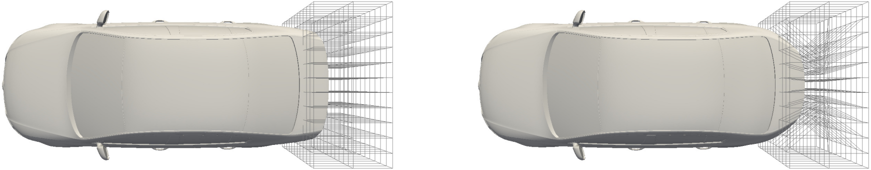

Aerodynamic shape design of automobile

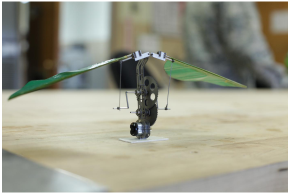
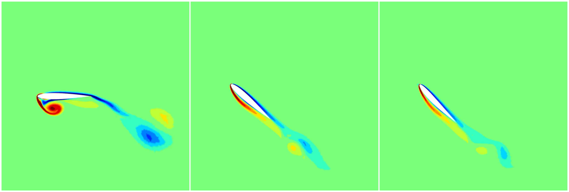

Optimal flapping motion of micro aerial vehicle

PDE optimization is ubiquitous in science and engineering

Control: Drive system to a desired state

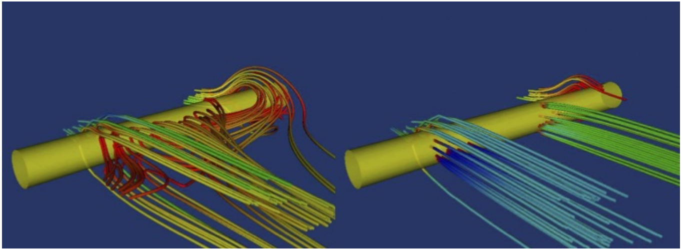

Boundary flow control

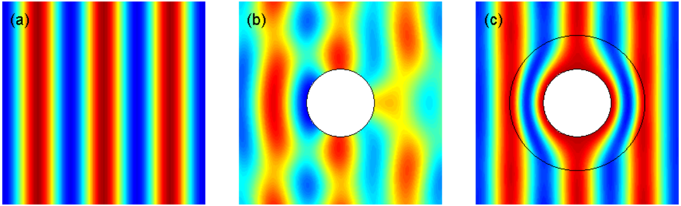

Metamaterial cloaking – electromagnetic invisibility

PDE optimization is ubiquitous in science and engineering

Inverse problems: Infer the problem setup given solution observations

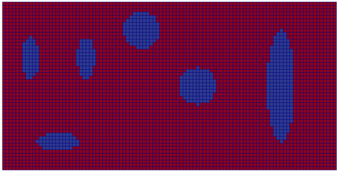

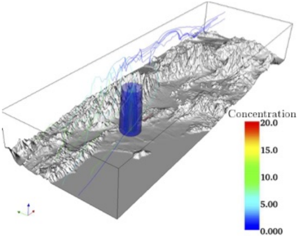

Material inversion: find inclusions from acoustic, structural measurements

Source inversion: find source of contaminant from downstream measurements

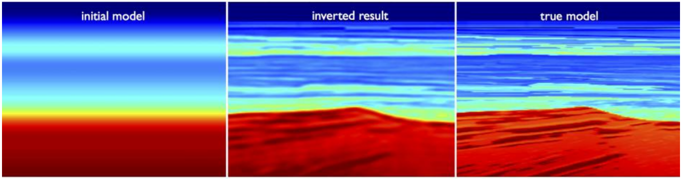

Full waveform inversion: estimate subsurface of crust from acoustic measurements

Unsteady PDE-constrained optimization formulation

Goal: Find the solution of the *unsteady PDE-constrained optimization* problem

$$
\begin{aligned}
\underset{\boldsymbol{U},\ \boldsymbol{\mu}}{\text{minimize}} \quad & \mathcal{J}(\boldsymbol{U}, \boldsymbol{\mu}) \\
\text{subject to} \quad & \boldsymbol{C}(\boldsymbol{U}, \boldsymbol{\mu}) \leq 0 \\
& \frac{\partial \boldsymbol{U}}{\partial t} + \nabla \cdot \boldsymbol{F}(\boldsymbol{U}, \nabla \boldsymbol{U}) = 0 \ \text{ in } \ v(\boldsymbol{\mu}, t)
\end{aligned}
$$

$\boldsymbol{U}(\boldsymbol{x}, t)$	PDE solution
$\boldsymbol{\mu}$	design/control parameters
$\mathcal{J}(\boldsymbol{U}, \boldsymbol{\mu}) = \int_{T_0}^{T_f} \int_{\boldsymbol{\Gamma}} j(\boldsymbol{U}, \boldsymbol{\mu}, t)\, dS\, dt$	objective function
$\boldsymbol{C}(\boldsymbol{U}, \boldsymbol{\mu}) = \int_{T_0}^{T_f} \int_{\boldsymbol{\Gamma}} \mathbf{c}(\boldsymbol{U}, \boldsymbol{\mu}, t)\, dS\, dt$	constraints

Nested approach to PDE-constrained optimization

Optimizer

Primal PDE

Dual PDE

Nested approach to PDE-constrained optimization

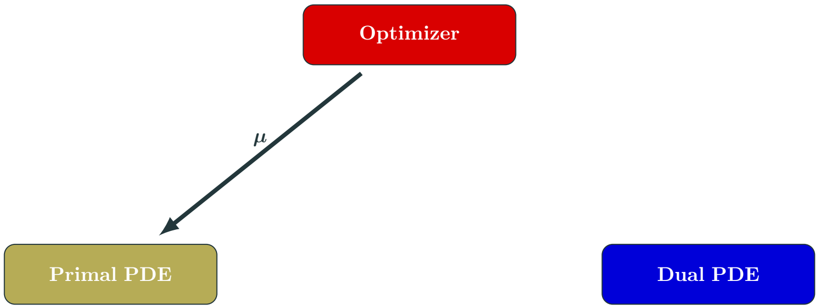

Nested approach to PDE-constrained optimization

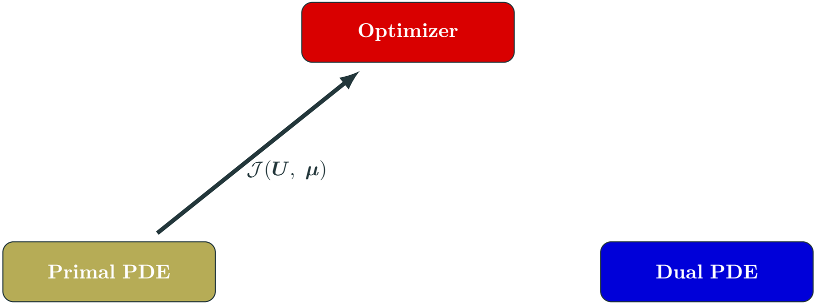

Nested approach to PDE-constrained optimization

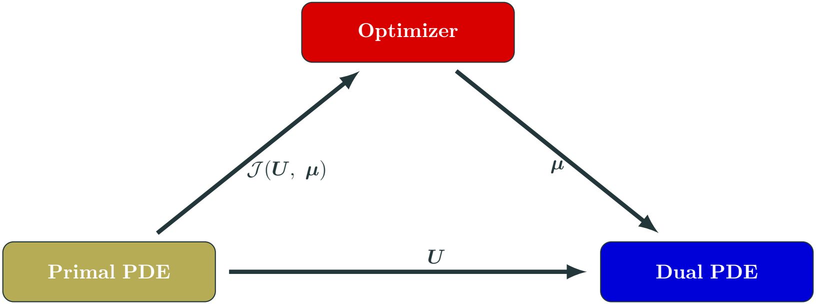

Nested approach to PDE-constrained optimization

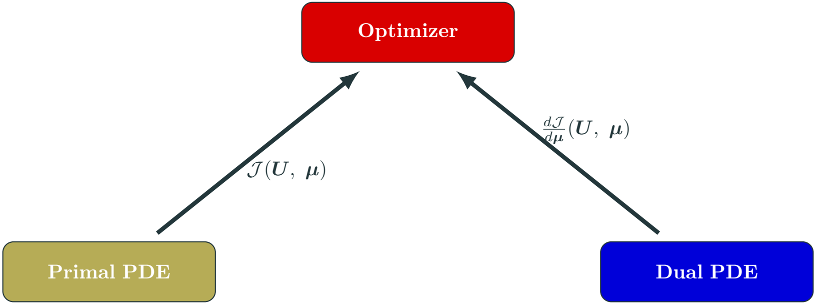

High-order discretization of PDE-constrained optimization

- *Continuous* PDE-constrained optimization problem

$$\begin{aligned}
\underset{\boldsymbol{U},\ \boldsymbol{\mu}}{\text{minimize}} \quad & \mathcal{J}(\boldsymbol{U}, \boldsymbol{\mu}) \\
\text{subject to} \quad & \boldsymbol{C}(\boldsymbol{U}, \boldsymbol{\mu}) \leq 0 \\
& \frac{\partial \boldsymbol{U}}{\partial t} + \nabla \cdot \boldsymbol{F}(\boldsymbol{U}, \nabla \boldsymbol{U}) = 0 \quad \text{in} \quad v(\boldsymbol{\mu}, t)
\end{aligned}$$

- *Fully discrete* PDE-constrained optimization problem

$$\begin{aligned}
\underset{\substack{\boldsymbol{u}_0,\ \dots,\ \boldsymbol{u}_{N_t} \in \mathbb{R}^{N_{\boldsymbol{u}}},\\ \boldsymbol{k}_{1,1},\ \dots,\ \boldsymbol{k}_{N_t,s} \in \mathbb{R}^{N_{\boldsymbol{u}}},\\ \boldsymbol{\mu} \in \mathbb{R}^{n_{\boldsymbol{\mu}}}}}{\text{minimize}} \quad & J(\boldsymbol{u}_0,\ \dots,\ \boldsymbol{u}_{N_t},\ \boldsymbol{k}_{1,1},\ \dots,\ \boldsymbol{k}_{N_t,s},\ \boldsymbol{\mu}) \\
\text{subject to} \quad & \mathbf{C}(\boldsymbol{u}_0,\ \dots,\ \boldsymbol{u}_{N_t},\ \boldsymbol{k}_{1,1},\ \dots,\ \boldsymbol{k}_{N_t,s},\ \boldsymbol{\mu}) \leq 0 \\
& \boldsymbol{u}_0 - \boldsymbol{g}(\boldsymbol{\mu}) = 0 \\
& \boldsymbol{u}_n - \boldsymbol{u}_{n-1} - \sum_{i=1}^{s} b_i \boldsymbol{k}_{n,i} = 0 \\
& \boldsymbol{M}\boldsymbol{k}_{n,i} - \Delta t_n \boldsymbol{r}\left(\boldsymbol{u}_{n,i},\ \boldsymbol{\mu},\ t_{n,i}\right) = 0
\end{aligned}$$

Optimal rigid body motion (RBM), time-morph geometry (TMG)

Energy = 9.4096	Energy = 4.9476	Energy = 4.6182
Thrust = 0.1766	Thrust = 2.500	Thrust = 2.500

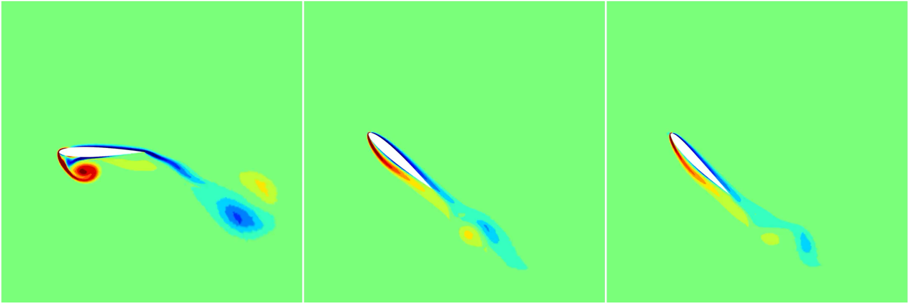

Initial Guess	Optimal RBM	Optimal RBM/TMG
	$T_x = 2.5$	$T_x = 2.5$

Energetically optimal flapping in three dimensions

Energy = 1.4459e-01
Thrust = -1.1192e-01

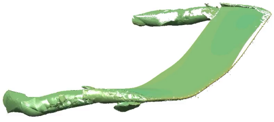

Energy = 3.1378e-01
Thrust = 0.0000e+00

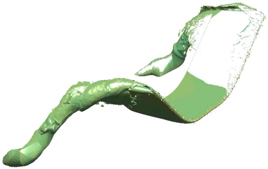

Energetically optimal flapping vs. required thrust

Energy $= 1.8445$
Thrust $= 0.06729$

Initial Guess

Energy $= 0.21934$
Thrust $= 0.0000$

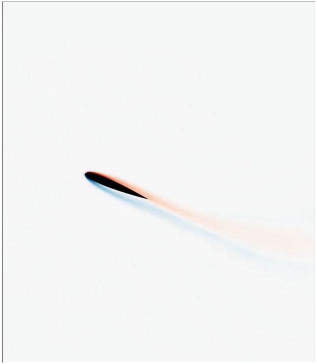

Optimal
$T_x = 0$

Energy $= 6.2869$
Thrust $= 2.5000$

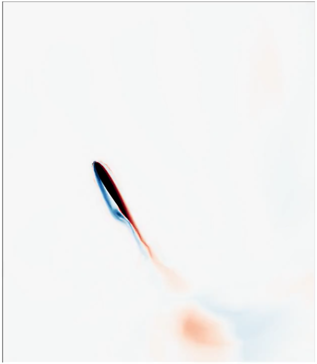

Optimal
$T_x = 2.5$

Energetically optimal flapping vs. required thrust: QoI

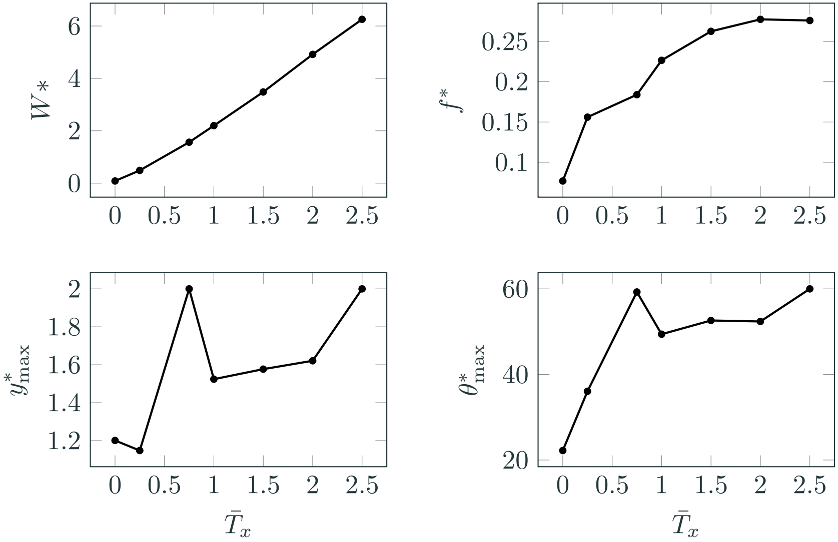

The optimal flapping energy (W^*), frequency (f^*), maximum heaving amplitude ($y^*_{\max}$), and maximum pitching amplitude ($\theta^*_{\max}$) as a function of the thrust constraint $\bar{T}_x$.

Current MRI 4D flow reconstruction: insufficient for infants

- Resolution: 3mm, 25-100ms in 10-20 minute scan
- Greater resolution = more noise, longer scan
- Biomarkers (WSS) must be computed from noisy velocity measurements
- Still very far from resolution needed for congenital heart disease

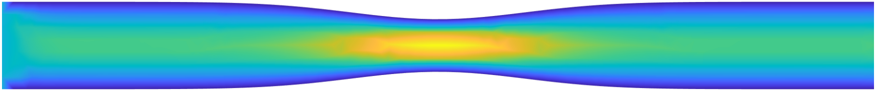

True *in vivo* flow

Current MRI 4D flow reconstruction: insufficient for infants

- Resolution: 3mm, 25-100ms in 10-20 minute scan
- Greater resolution = more noise, longer scan
- Biomarkers (WSS) must be computed from noisy velocity measurements
- Still very far from resolution needed for congenital heart disease

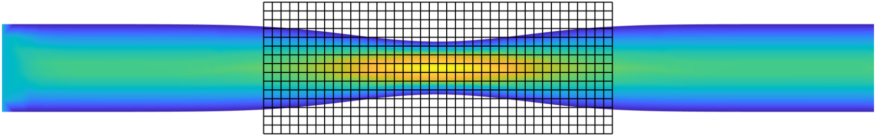

MRI protocol

Current MRI 4D flow reconstruction: insufficient for infants

- Resolution: 3mm, 25-100ms in 10-20 minute scan
- Greater resolution = more noise, longer scan
- Biomarkers (WSS) must be computed from noisy velocity measurements
- Still very far from resolution needed for congenital heart disease

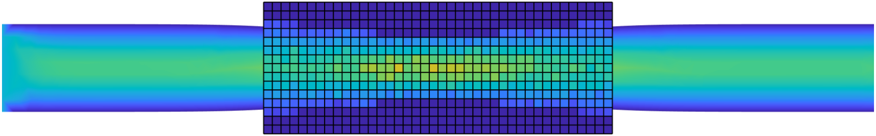

MRI measurements: noisy, space-time averages over voxels

Current MRI 4D flow reconstruction: insufficient for infants

- Resolution: 3mm, 25-100ms in 10-20 minute scan
- Greater resolution = more noise, longer scan
- Biomarkers (WSS) must be computed from noisy velocity measurements
- Still very far from resolution needed for congenital heart disease

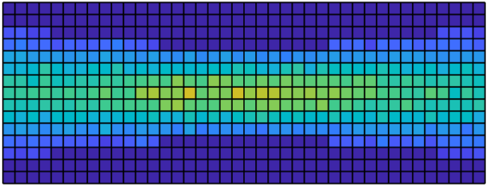

MRI measurements: noisy, space-time averages over voxels

Current MRI 4D flow reconstruction: insufficient for infants

- Resolution: 3mm, 25-100ms in 10-20 minute scan
- Greater resolution = more noise, longer scan
- Biomarkers (WSS) must be computed from noisy velocity measurements
- Still very far from resolution needed for congenital heart disease

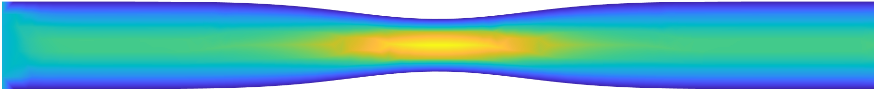

Improve with CFD:

Current MRI 4D flow reconstruction: insufficient for infants

- Resolution: 3mm, 25-100ms in 10-20 minute scan
- Greater resolution = more noise, longer scan
- Biomarkers (WSS) must be computed from noisy velocity measurements
- Still very far from resolution needed for congenital heart disease

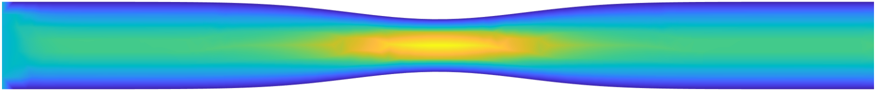

Improve with CFD: BCs? ICs? material properties?

In vivo image reconstruction using *all* prior knowledge

To break *resolution-noise barrier*, we incorporate all available information into reconstruction procedure

- geometry of patient-specific flow domain
- conservation of mass, momentum, energy (Navier-Stokes)
- low-resolution *in vivo* flow measurements (MRI data)

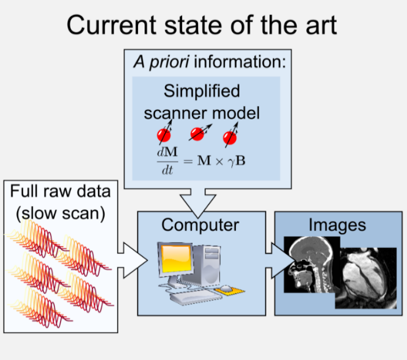

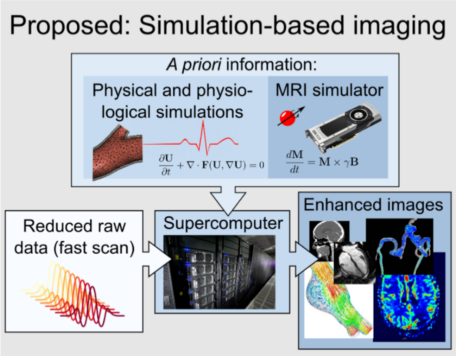

Simulation-based imaging

- Phase I: Collect MRI data to extract flow domain and 4D flow measurements
- Phase II: Image segmentation and mesh generation
- Phase III: Find Navier-Stokes solution that best explains flow data (PDE-constrained optimization to minimize MRI data misfit)

$$\begin{aligned} \underset{\boldsymbol{U},\ \boldsymbol{\mu}}{\text{minimize}} \quad & \mathcal{J}(\boldsymbol{U}) \\ \text{subject to} \quad & \frac{\partial \boldsymbol{U}}{\partial t} + \nabla \cdot \boldsymbol{F}(\boldsymbol{U}, \nabla \boldsymbol{U}, \boldsymbol{\mu}) = 0 \end{aligned}$$

$\boldsymbol{U}$	:	PDE solution
$\boldsymbol{\mu}$	:	BCs, IC, material properties
$\mathcal{J}(\boldsymbol{U})$	:	CFD/MRI misfit function
$\boldsymbol{F}(\boldsymbol{U}, \nabla \boldsymbol{U}, \boldsymbol{\mu})$	:	Navier-Stokes flux function

- Phase IV: Visualize solution and compute biomarkers

Simulation-based imaging workflow

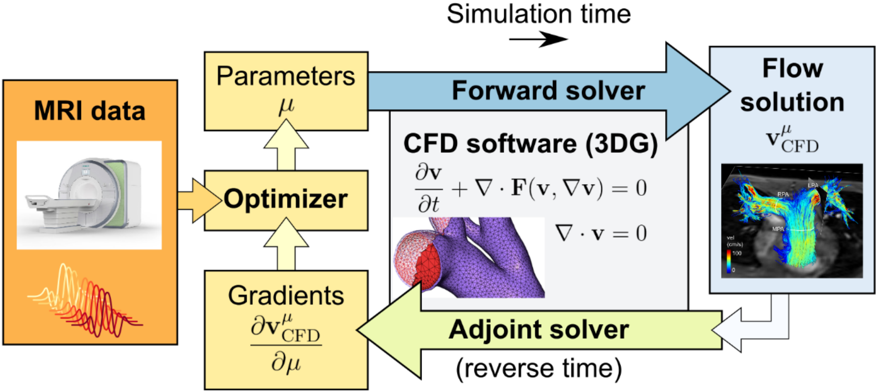

Phantom validation: laser PIV vs. 4D flow MRI vs. SBI

- Experimental setup: water tank with pulsatile inflow
- Precise laser PIV measurements: “true” flow
- Compare standard 4D flow MRI (high-res) and SBI with laser PIV “truth”
- SBI uses low-resolution MRI data

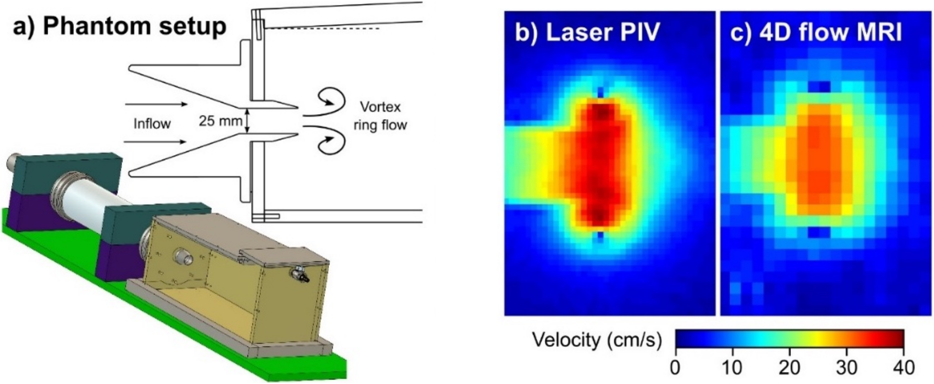

SBI captures features that cannot be resolved with 4D flow MRI

- Resolution of high-resolution 4D flow MRI: $3 \times 3 \times 3\text{mm}^3$, 50ms
- Resolution of low-resolution 4D flow MRI used for SBI: $6 \times 6 \times 6\text{mm}^3$, 100ms

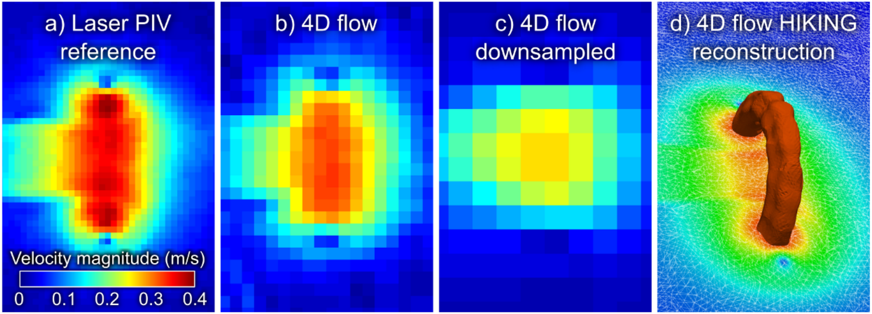

High-quality reconstruction with experimental data: pulsatile flow

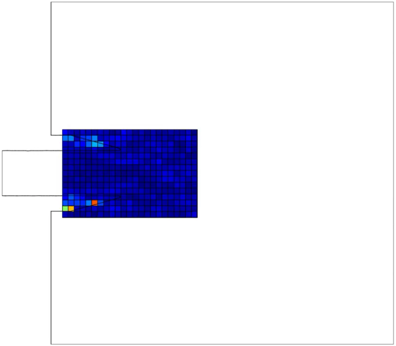

MRI data

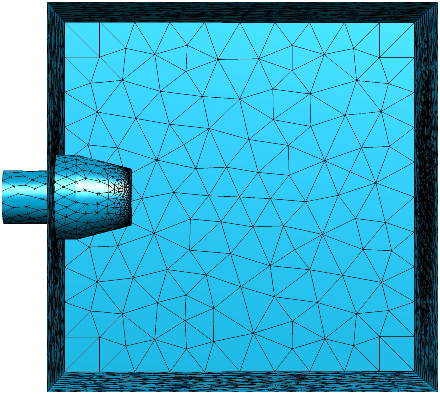

Reconstructed flow

In vivo test of SBI flow reconstruction: Circle of Willis

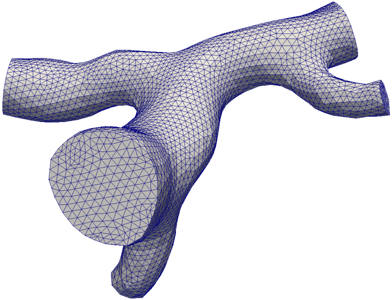

Patient-specific mesh of brain vessel network (Circle of Willis)

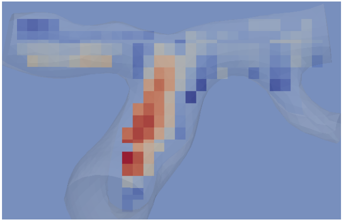

MRI voxel velocity data on 2D spatial slice at time instance

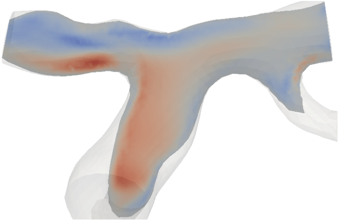

SBI reconstruction

Streamlines of flow: MRI 4D flow vs SBI reconstruction

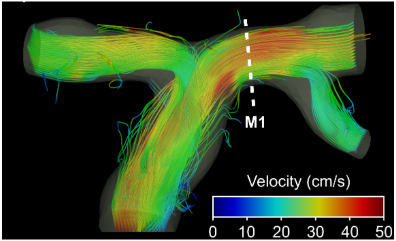

4D flow MRI reconstruction

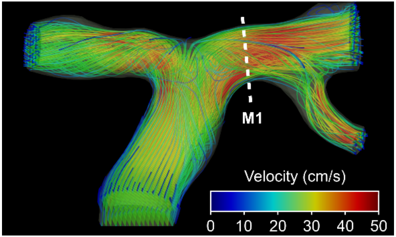

SBI reconstruction

SBI matches reference velocity measurements better than 4D flow MRI even for *in vivo* application

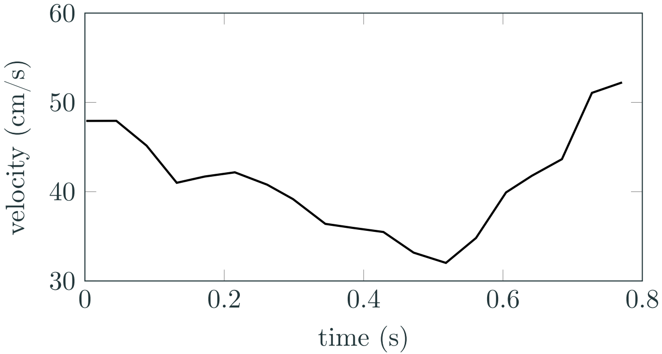

The reconstructed flow field (-·-·-) provides better agreement to accurate velocity measurements (——) on a 2D section than the 4D flow MRI measurements (- - -)

SBI matches reference velocity measurements better than 4D flow MRI even for *in vivo* application

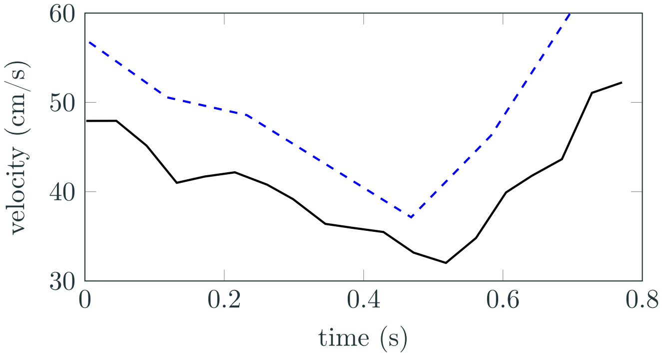

The reconstructed flow field (-·-·-) provides better agreement to accurate velocity measurements (——) on a 2D section than the 4D flow MRI measurements (- - -)

SBI matches reference velocity measurements better than 4D flow MRI even for *in vivo* application

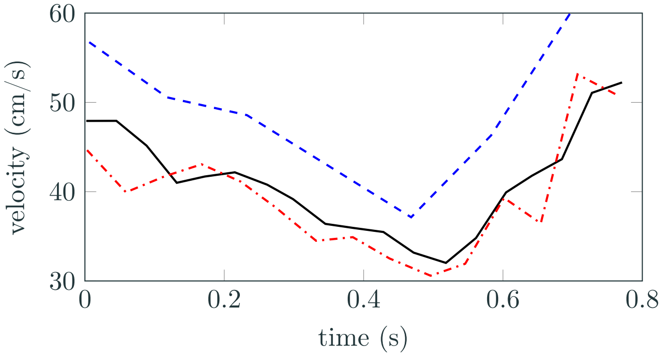

The reconstructed flow field (red dash-dotted line) provides better agreement to accurate velocity measurements (black solid line) on a 2D section than the 4D flow MRI measurements (blue dashed line)

State-of-the-art numerical methods for resolving shocks

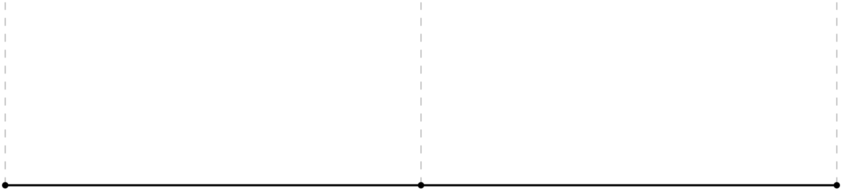

Fundamental issue: approximate discontinuity with polynomial basis

State-of-the-art numerical methods for resolving shocks

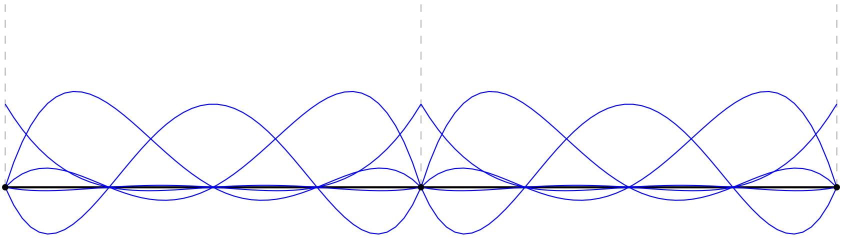

Fundamental issue: approximate discontinuity with polynomial basis

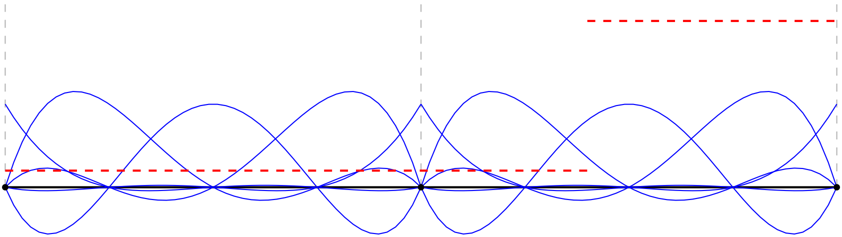

Fundamental issue: approximate discontinuity with polynomial basis

State-of-the-art numerical methods for resolving shocks

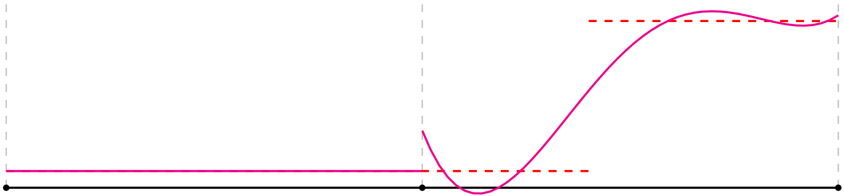

Fundamental issue: approximate discontinuity with polynomial basis

State-of-the-art numerical methods for resolving shocks

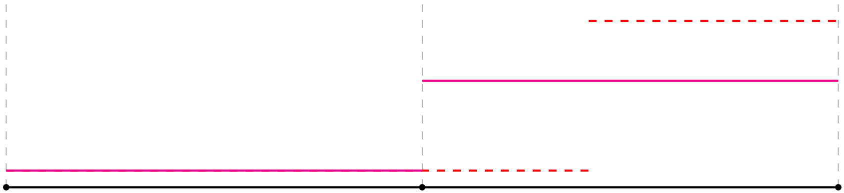

Fundamental issue: approximate discontinuity with polynomial basis

Exising solutions: **limiting**, artificial viscosity

Drawbacks: order reduction, local refinement

State-of-the-art numerical methods for resolving shocks

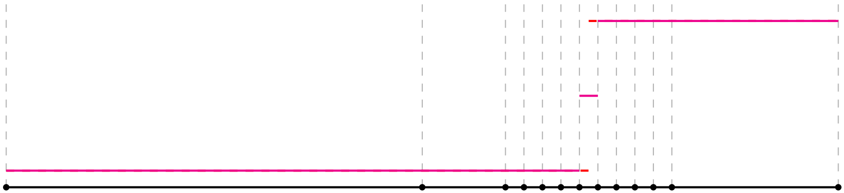

Fundamental issue: approximate discontinuity with polynomial basis

Exising solutions: **limiting**, artificial viscosity

Drawbacks: order reduction, local refinement

State-of-the-art numerical methods for resolving shocks

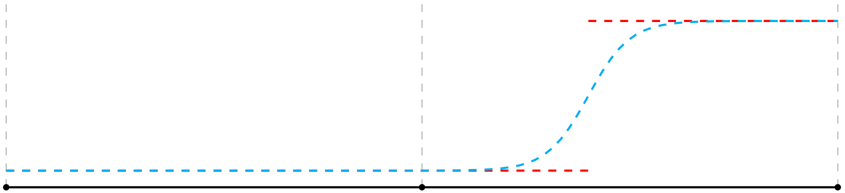

Fundamental issue: approximate discontinuity with polynomial basis

Exising solutions: limiting, **artificial viscosity**

Drawbacks: order reduction, local refinement

State-of-the-art numerical methods for resolving shocks

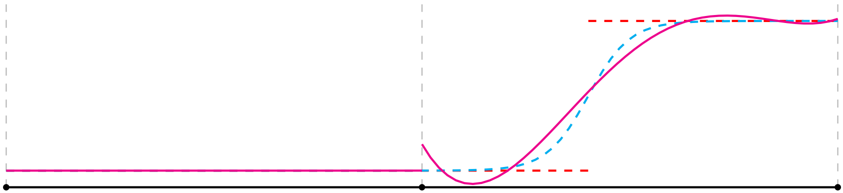

Fundamental issue: approximate discontinuity with polynomial basis

Exising solutions: limiting, **artificial viscosity**

Drawbacks: order reduction, local refinement

State-of-the-art numerical methods for resolving shocks

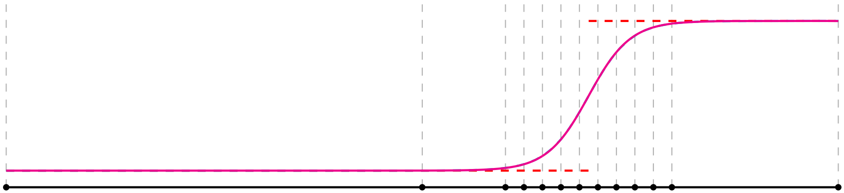

Fundamental issue: approximate discontinuity with polynomial basis

Exising solutions: limiting, **artificial viscosity**

Drawbacks: order reduction, local refinement

State-of-the-art numerical methods for resolving shocks

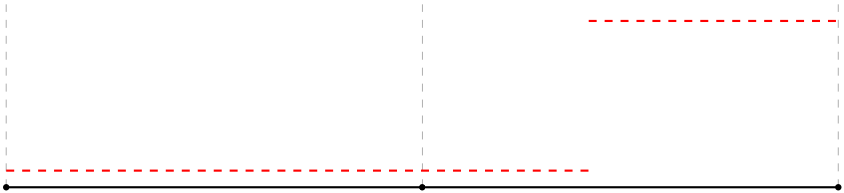

Fundamental issue: approximate discontinuity with polynomial basis

Exising solutions: limiting, artificial viscosity

Drawbacks: order reduction, local refinement

Proposed solution: align features of solution basis with features in the solution using optimization formulation and solver

State-of-the-art numerical methods for resolving shocks

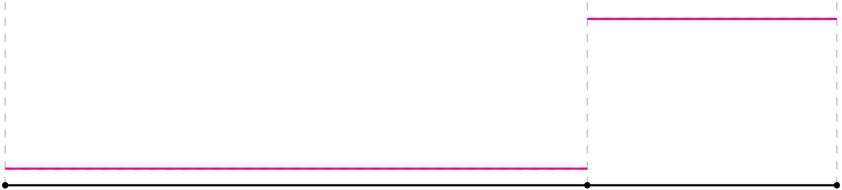

Fundamental issue: approximate discontinuity with polynomial basis

Exising solutions: limiting, artificial viscosity

Drawbacks: order reduction, local refinement

Proposed solution: align features of solution basis with features in the solution using optimization formulation and solver

Tracking method for stable, high-order resolution of discontinuities

Goal: Align element faces with (unknown) discontinuities to perfectly capture them and approximate smooth regions to high-order

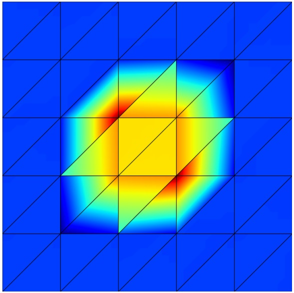

Non-aligned

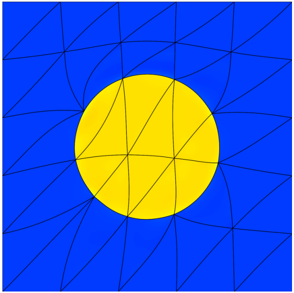

Discontinuity-aligned

Tracking method for stable, high-order resolution of discontinuities

Goal: Align element faces with (unknown) discontinuities to perfectly capture them and approximate smooth regions to high-order

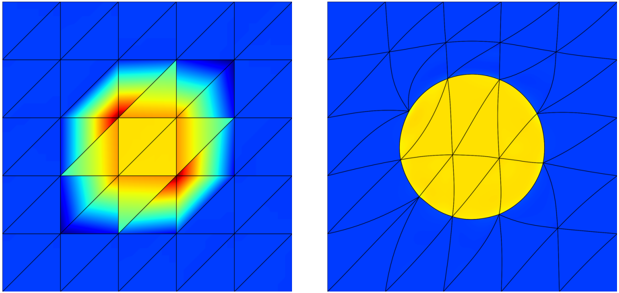

Non-aligned Discontinuity-aligned

Ingredients

- Discontinuous Galerkin discretization: inter-element jumps, high-order
- Discontinuity-aligned mesh is the solution of an optimization problem constrained by the discrete PDE $\implies$ **implicit shock tracking**
- Full space solver that converges the solution and mesh simultaneously to ensure solution of PDE never required on non-aligned mesh

Why tracking: Recover optimal $\mathcal{O}(h^{p+1})$ convergence rates

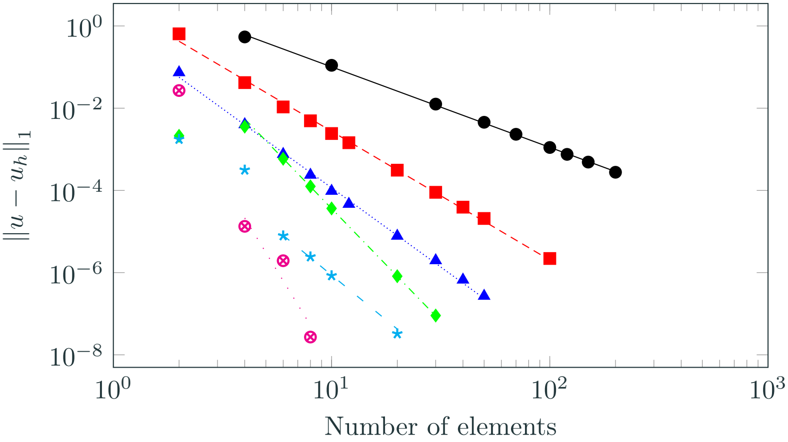

Convergence of DG discretization with implicit shock tracking for the modified inviscid Burgers' equation for polynomial orders $p = 1$ (●), $p = 2$ (■), $p = 3$ (▲), $p = 4$ (♦), $p = 5$ ($\ast$), $p = 6$ ($\otimes$). The slopes of the best-fit lines to the data points in the asymptotic regime are: $\angle -1.95$ (——), $\angle -3.13$ (- - - -), $\angle -3.85$ (⋯⋯), $\angle -5.47$ (-·-·-), $\angle -4.36$ (– –), $\angle -8.67$ (· · ·).

Why high-order tracking: Benefits more dramatic than low-order

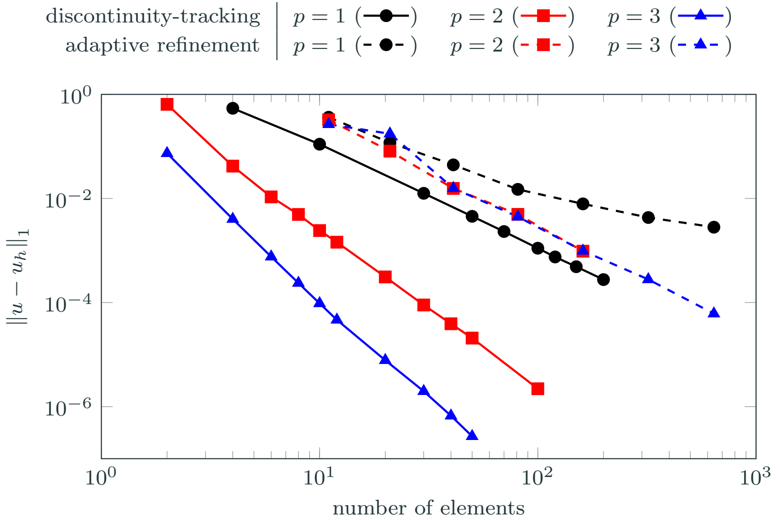

Key observation: Accuracy improvement of tracking approach relative to (specialized) adaptive mesh refinement is more exaggerated for high-order approximations: $\mathcal{O}(10^1)$ for $p = 1$ and $\mathcal{O}(10^6)$ for $p = 3$.

Why high-order tracking: Accurate solutions on coarse meshes

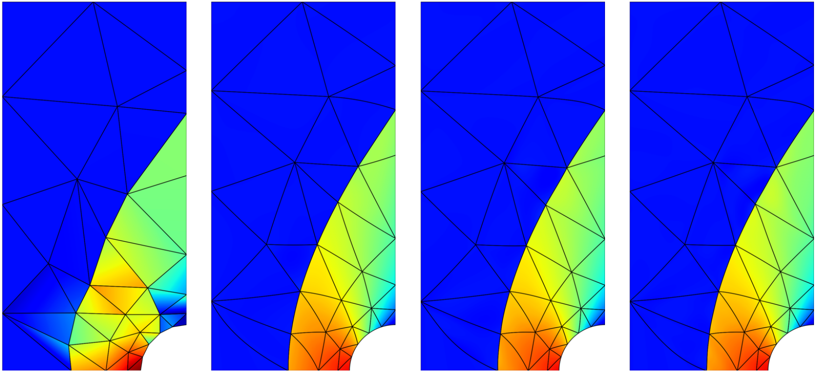

Density of supersonic flow ($M = 2$) past a cylinder using implicit shock tracking with $p = 1$ to $p = 4$ (left to right) DG discretization.

Key observation: High-order tracking enables accurate resolution of 2D supersonic flow with 48 elements; the error in the stagnation enthalpy is $\mathcal{O}(10^{-4})$ for $p = 2$ (1152 DoF).

Why high-order tracking: Accurate solutions on coarse meshes

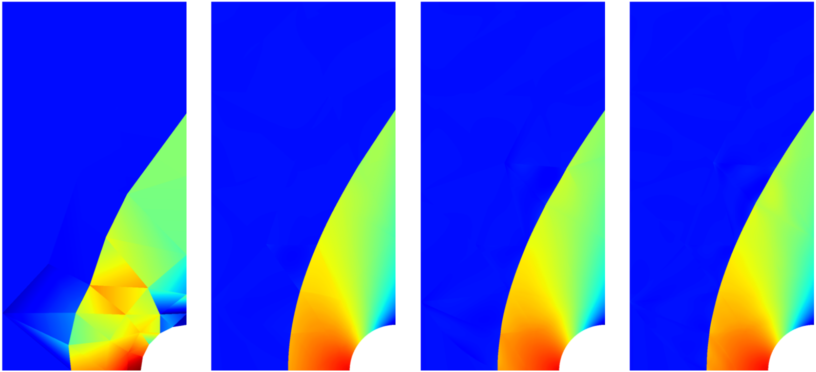

Density of supersonic flow ($M = 2$) past a cylinder using implicit shock tracking with $p = 1$ to $p = 4$ (left to right) DG discretization.

Key observation: High-order tracking enables accurate resolution of 2D supersonic flow with 48 elements; the error in the stagnation enthalpy is $\mathcal{O}(10^{-4})$ for $p = 2$ (1152 DoF).

Why not tracking: Difficult for complex discontinuity surfaces

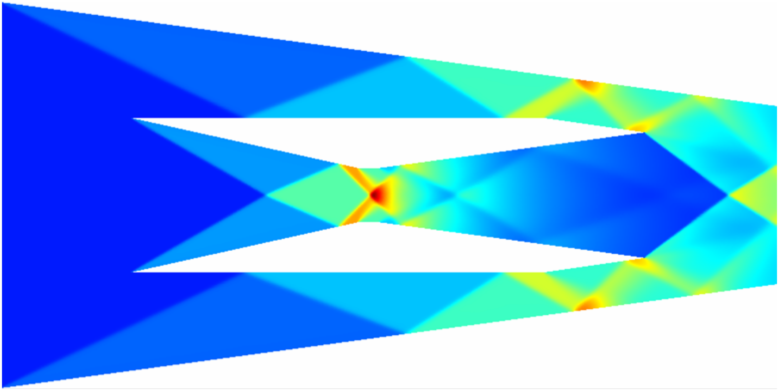

Implicit shock tracking

Aims to overcome the difficulty of explicitly meshing the unknown shock surface

Linear advection, trigonometic shock

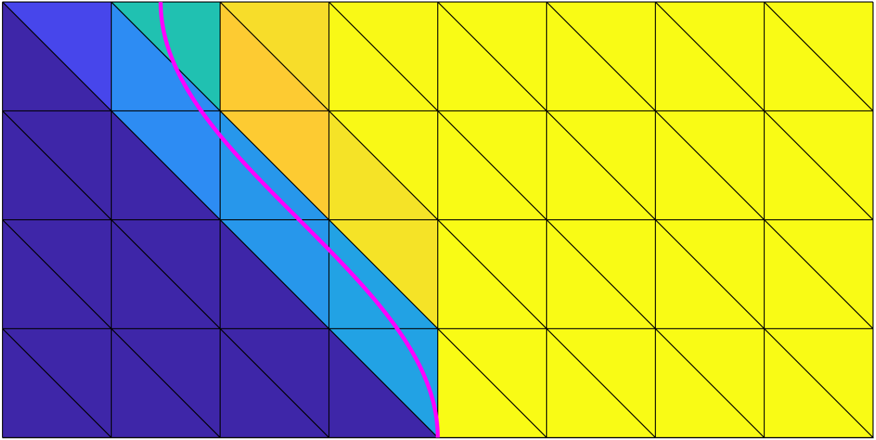

$p = 0$ space for solution, $q = 2$ space for mesh

L_1 error $= 1.15 \times 10^{-3}$

Inviscid Burgers' equation: space-time formulation

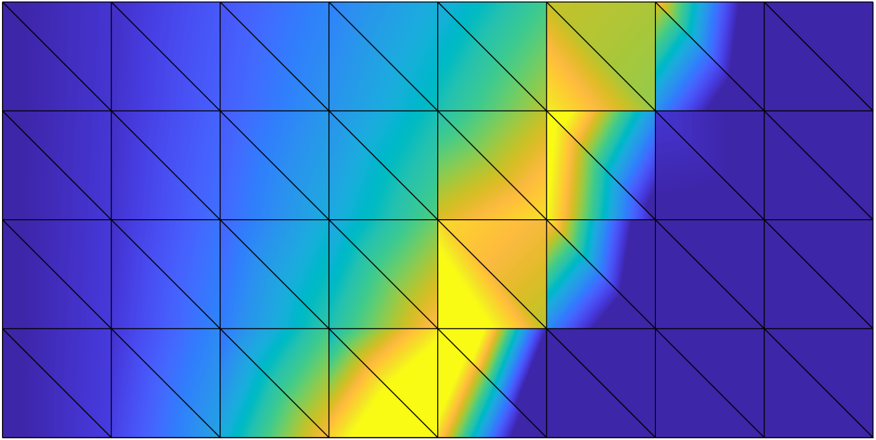

$p = 0$ space for solution, $q = 3$ space for mesh

Supersonic flow past wedge ($M = 2$)

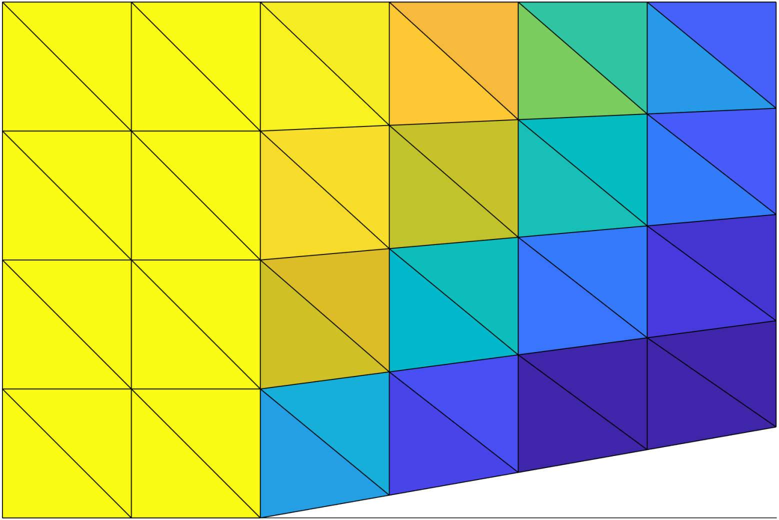

$p = 0$ space for solution, $q = 1$ space for mesh

L^2 stagnation enthalpy error: 7.94×10^{-10}

Supersonic flow past NACA0012 airfoil ($M = 1.5$)

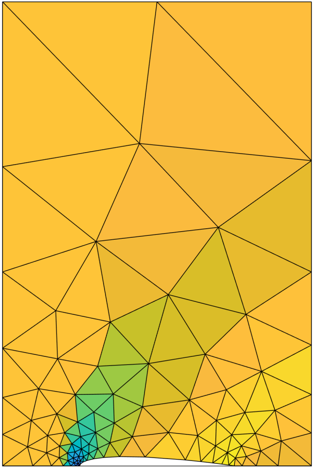

Initialization

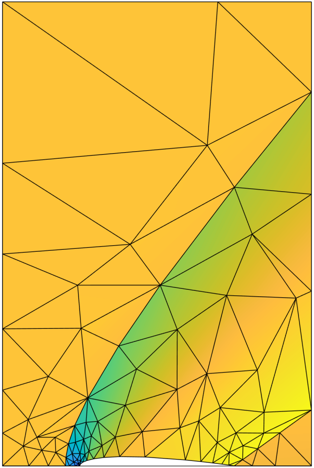

$p = 1$ tracking
$e_H = 1.30 \times 10^{-3}$

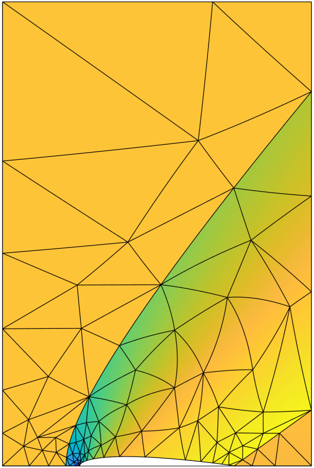

$p = 2$ tracking
$e_H = 6.73 \times 10^{-5}$

Supersonic flow past NACA0012 airfoil ($M = 1.5$)

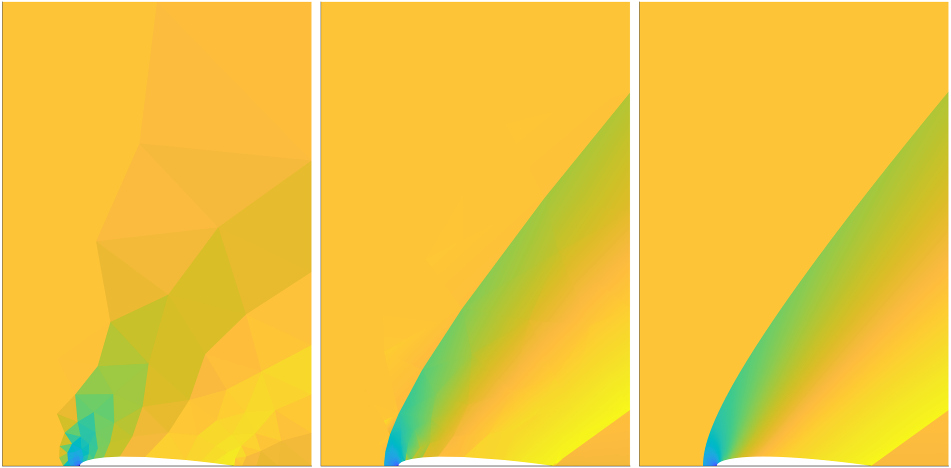

Initialization | $p = 1$ tracking, $e_H = 1.30 \times 10^{-3}$ | $p = 2$ tracking, $e_H = 6.73 \times 10^{-5}$

Transonic flow past NACA0012 airfoil ($M = 0.85$)

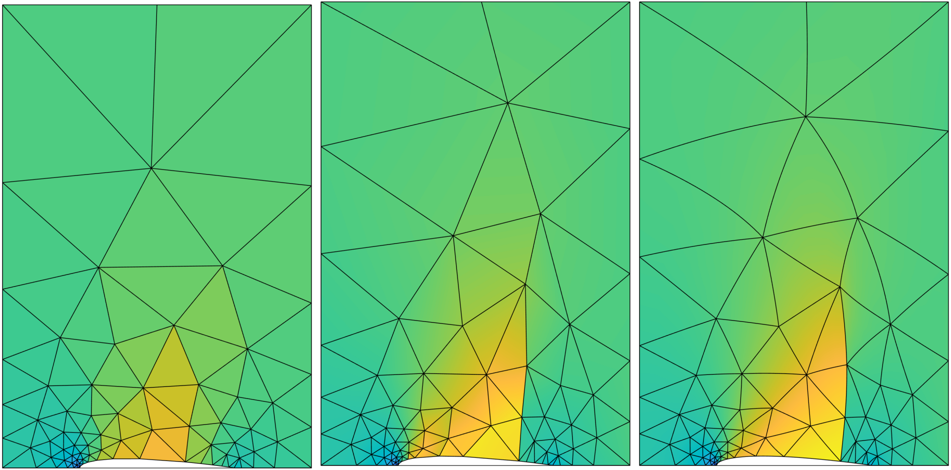

Initialization $\quad$ $p = 1$ tracking $\quad$ $p = 2$ tracking

Transonic flow past NACA0012 airfoil ($M = 0.85$)

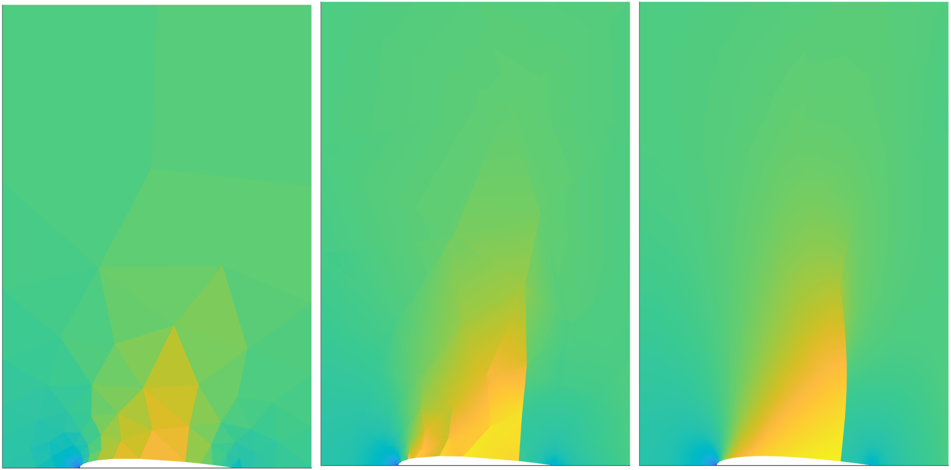

Initialization $\quad$ $p = 1$ tracking $\quad$ $p = 2$ tracking